Appendix: Enchained growth and cluster dislocation : a possible mechanism for microbiota homeostasis

Florence Bansept[1], Kathrin Schumann-Moor[2,3], Médéric Diard[2], Wolf-Dietrich Hardt[2], Emma Slack[2], and Claude Loverdo[1,*]

[1]Laboratoire Jean Perrin, Sorbonne Université / CNRS, Paris, France.
[2]Institute of Microbiology, ETH Zürich, Zürich, Switzerland.
[3]Present address: Center of Dental Medicine / Oral and Maxillofacial Surgery, University of Zürich, Switzerland
[*]Corresponding author

1 Order of magnitude of the encounter time between two bacteria

The typical time to find one target of radius a in a sphere of radius b by diffusion is of the order of $b^3/(Da)$, so the typical time when there are N bacteria in a volume V is of the order of $V/(NDa)$. For bacteria, a is in the micrometer range. Bacteria typically swim at $10\mu m/s$, and change direction every second, which gives a diffusion coefficient of the order of $10^{-10}m^2/s$ (The peristaltic motions of the digesta are large scale movement rather than local diffusion, so we assume they have a smaller effect on diffusion). The mouse's cecum has a volume of the order of $(1\text{cm})^3$. In experiments of [1], the smallest inoculum consists in $N = 10^5$ bacteria, which is already large compared to what could be a realistic number of pathogenic bacteria in food poisoning (10^5 is the typical number of *Salmonella* for food poisoning in humans [2], which are much larger than mice). With these numbers, the typical encounter time is of the order of $10^5 s$, i.e 30h, about 10 times longer than the typical digestion time in mice.

2 Argument for a low escape probability

When a bacteria replicates, the time for septation is of the order of a few minutes. We intuitively think that this time is much larger than the time required for bacteria to stick when they randomly meet. The aim of this section is to give an overestimate of the typical time τ_k it takes for a bacteria to stick to another when they meet.

We use the data on figure 1k of [1] about non-dividing bacteria (so the only sticking is from random encounters). The majority of them are aggregated after

a few hours for a concentration of $10^7 - 10^8$ bacteria. As we will calculate an overestimate of τ_k, we take the highest concentration and the minimum time, i.e. $N = 10^8$ bacteria in $V = 1cm^3$ and $\tau_{exp} = 1hour$.

If the diffusion coefficient is high enough, the time for bacteria to stick to each other will be limited by the rate k at which bacteria stick to each other when they are in close vicinity. k is the inverse of τ_k. If the diffusion coefficient is smaller, then the time to first encounter will also play a role, but as we calculate an overestimate of τ_k, we can neglect this.

The bacteria typical size is a few micrometers, $4\mu m$ is an overestimate of the maximum bacterial size. To be in close contact, two bacteria must be at at most $a = 4\mu m$ away. Let us assume that then the volume of possible contact is $4/3\pi a^3$, which is an overestimate, because only certain orientations will allow bacteria to touch each other. Then, the proportion of time spent in close contact will be of the order of $(N4\pi a^3)/(3V)$. Then the typical time to stick to each other will be $\tau_{exp} = \tau_k 3V/(N4\pi a^3)$. Then $\tau_k = \tau_{exp} N4\pi a^3/(3V)$. Numerically, we obtain less than $100s$ as an overestimate of τ_k.

Thus, this confirms that when septation takes several minutes, the probability for bacteria to escape enchainment is very small, which justifies that we take in general the limit of no escape.

3 Model with bacterial escape ($\delta > 0$) and differential loss ($c \neq c'$).

Figure 1 shows how the growth rate depends on r for different δ, δ', δ'', c and c'.

We detail here how to obtain the approximation for the cluster size distribution. In the long time limit, the number of clusters of size i is of the order of $b_i \exp(\lambda t)$, with λ the largest eigenvalue. Equation (8) of main text simplifies to:

$$\lambda b_i = r(2\delta' - i)b_i + rb_{i-1}(i - 1 - 2\delta' + 3\delta'' - i\delta'') - (i-1)b_i\alpha + 2\alpha b_{i+1} - c'b_i \quad (1)$$

Assuming that i is large,

$$b_i \simeq (1 - \delta'')\frac{r}{r+\alpha} b_{i-1} \quad (2)$$

is required. Using this approximation for all i, the probability that a randomly chosen chain is of size k is:

$$p_k = \left(1 - (1-\delta'')\frac{r}{r+\alpha}\right)\left((1-\delta'')\frac{r}{r+\alpha}\right)^{k-1} \quad (3)$$

Free bacteria are released at a rate $2r\delta' + 2\alpha$ per cluster. This rate is independent of the cluster size. The direct contributions to the increase of free bacteria from clusters of size i compared to all the larger clusters will be (with $K = (1-\delta'')r/(r+\alpha)$):

$$\frac{contribution\ larger}{contribution\ i} = \frac{(2r\delta' + 2\alpha)\sum_{j=i+1}^{\infty}(1-K)K^j}{(2r\delta' + 2\alpha)(1-K)K^i} = \sum_{j=1}^{\infty} K^j = \frac{K}{1-K} = \frac{(1-\delta'')r}{\alpha + r\delta''} \quad (4)$$

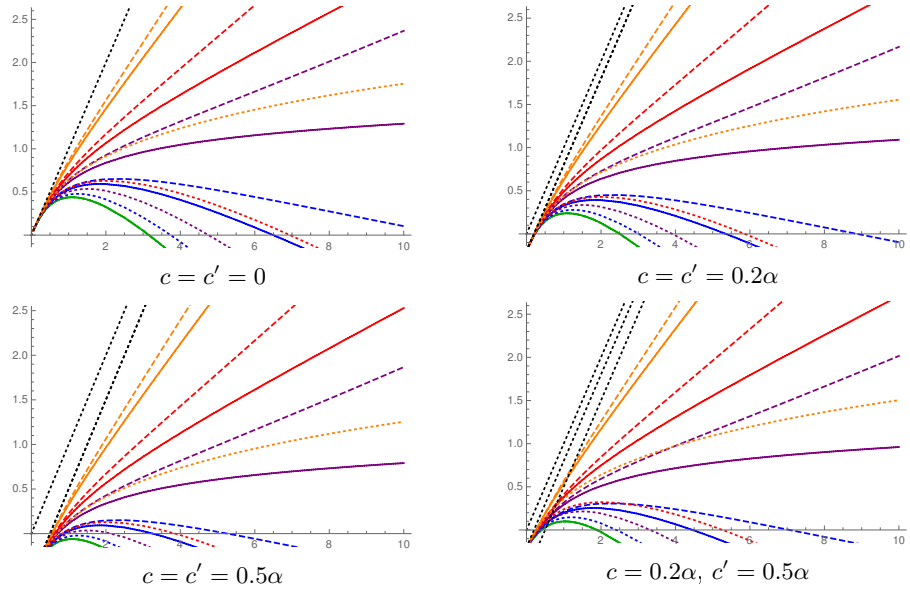

Figure 1: Growth rate λ as a function of the replication rate r, both in units of α. Numerical results (colors), with $\delta = \delta' = \delta''$ (solid lines), $\delta = \delta'$, and $\delta'' = 0$ (dashed lines), $\delta' = \delta'' = 0$ (dotted lines). $\delta =$ 0, 0.1, 0.2, 0.3, 0.5. The black dotted lines are either r/α, $(r-c)/\alpha$ or $(r-c')/\alpha$. As expected, if $c = c'$, the resulting growth rate are the same than when $c = c' = 0$, minus c. If $c \neq c'$, the results are closer for small r/α to the results if both c and c' had the c value. For the numerical results, $n_{max} = 40$.

If r is small compared to α (replication rate $\ll$ breaking rate), then this ratio is small. Thus the larger clusters are quickly negligible. Indeed, in this regime, clusters typically dislocate before new replications, so there are few larger clusters.

Figures 2, 3, 4, 5 show how the cluster size distribution depends on δ, δ', δ'', c and c'.

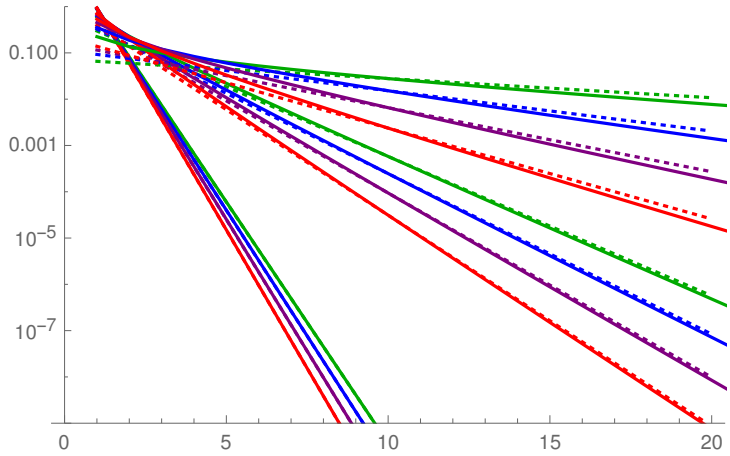

Figure 2: Distribution of the cluster sizes. All as in main figure 2B, except that the approximation (9) of main text is rescaled by the numerical value at $n = 10$. This shows that the approximation captures well the distribution of large clusters.

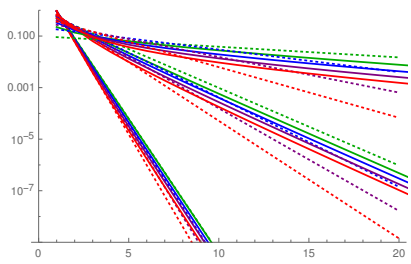

$\delta = \delta'$, $\delta'' = 0$

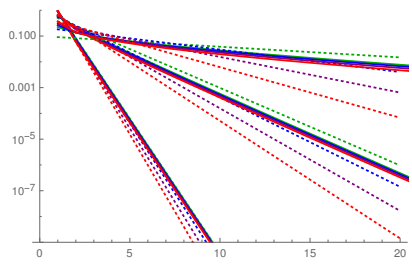

δ, $\delta' = \delta'' = 0$

Figure 3: Distribution of the cluster sizes. All as in figure 2D, except the values of δ' and δ''. The distribution is close to the result for $\delta = \delta' = \delta'' = 0$, which is in line with approximation (9) of main text which is independent of δ and δ'.

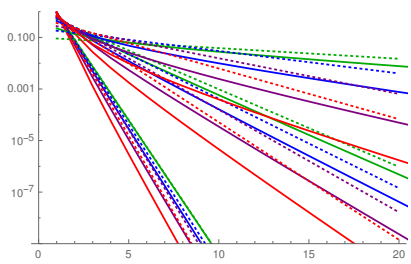

Dotted lines : approximation (9) of main text

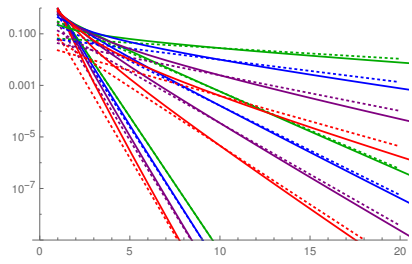

Dotted lines: approximation (9) of main text, rescaled by the numerical value at $n = 10$.

Figure 4: Distribution of the cluster sizes, for $\delta = \delta' = 2\delta''$. Other parameters as in figure 2D of main text. The approximation does not work as well as when $\delta = \delta' = \delta''$.

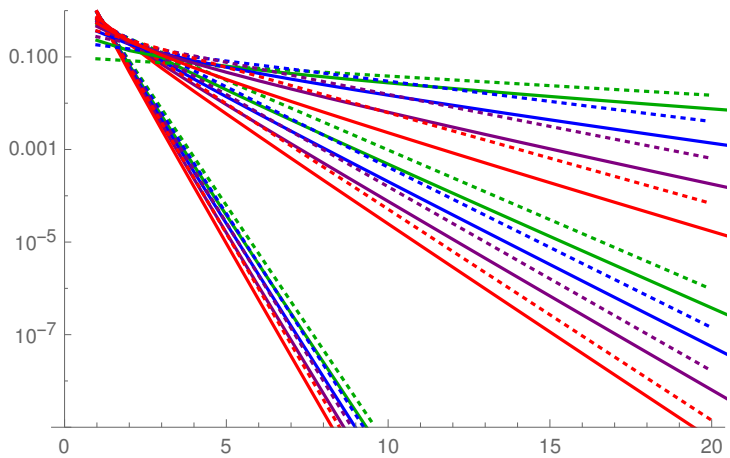

Figure 5: All as in figure 2D of main text, except $c = 0.2\alpha$, $c' = 0.5\alpha$. There is very little change in the cluster size distribution.

4 Chain length distribution with a fixed replication time - approximation

Below, we present in details the assumptions and calculations to obtain the approximation of the chain length distribution when bacteria replicate every τ.

We define $u(N,t)$ the number of chains of size N at t. Assuming N even,

$$u(N,t+\tau) = \sum_{i=0}^{\infty} q\left(\frac{N}{2}+i,t\right) l(N+2i,2i,\tau). \tag{5}$$

In the long time, $u(N,t) = f(N)\exp(\lambda t)$, with λ the long term growth rate, that is such that $\exp(\lambda\tau) = \mathcal{N}$, with $\mathcal{N}$ the largest eigenvalue of the matrix. Then previous equation, replacing $l(N+2i,2i,\tau)$ by its expression as in equation (11) of the main text, leads to:

$$\mathcal{N} f(N) = \sum_{i=0}^{\infty} f(\frac{N}{2}+i)\exp\left(-\alpha\tau\left(N-1+2i\right)\right)\left(\exp(\alpha\tau)-1\right)^{2i}\frac{2^{2i}}{(2i)!}. \tag{6}$$

We compare the 1st term of the sum to the rest of the sum. The first term is $f(\frac{N}{2})\exp\left(-\alpha\tau\left(N-1\right)\right)$, the rest of the sum is:

$$\sum_{i=1}^{\infty} f(\frac{N}{2}+i)\exp\left(-\alpha\tau\left(N-1+2i\right)\right)\left(\exp(\alpha\tau)-1\right)^{2i}\frac{2^{2i}}{(2i)!}. \tag{7}$$

We divide both by $\exp\left(-\alpha\tau\left(N-1\right)\right)$. Then this is equivalent of comparing $f(N/2)$ with:

$$S = \sum_{i=1}^{\infty} f(\frac{N}{2}+i)\exp\left(-2i\alpha\tau\right)\left(\exp(\alpha\tau)-1\right)^{2i}\frac{2^{2i}}{(2i)!}. \tag{8}$$

When $\alpha\tau$ is large, links typically break before the next replication, so there is little cluster formation, so it is expected that the chain length distribution decreases fast with N, so that for $i>0$, $f(\frac{N}{2}+i) \ll f(N/2)$. When $\alpha\tau$ is small, replication is slow compared to the typical time for one link to break. However, for a chain of length $N/2$, τ has to be compared to $(N/2-1)/\alpha$, the typical first link breaking time, thus for N large enough, we expect the number of large cluster to decrease, thus $f(\frac{N}{2}+i) \lesssim f(N/2)$ for $i>0$. We define B such as $f(\frac{N}{2}+i) \leq B, \forall i>0$. For $\alpha\tau$ large, $B \ll f(N/2)$, and for $\alpha\tau$ small, if N is large enough, $B \lesssim f(N/2)$. Then:

$$S \leq \sum_{i=1}^{\infty} B(1-\exp(-\alpha\tau))^{2i}\frac{2^{2i}}{(2i)!} = B\left(cosh\left(2(1-\exp(-\alpha\tau))\right)-1\right) \tag{9}$$

For $\alpha\tau$ large, $(cosh\left(2(1-\exp(-\alpha\tau))\right)-1) \simeq cosh(2)-1 \simeq 2.7$. For $\alpha\tau$ small, $(cosh\left(2(1-\exp(-\alpha\tau))\right)-1) \simeq 2(\alpha\tau)^2 \ll 1$.

Thus in the case of $\alpha\tau$ large, S is small relative to $f(N/2)$ because S is smaller than a few units times B, with B much smaller than $f(N/2)$. In the case of $\alpha\tau$ small, S is small relative to $f(N/2)$ because S is of the order of

$(\alpha\tau)^2 B$, with B of the order of $f(N/2)$. Then this justifies the assumption that only the first term of the sum matters:

$$f(N) \simeq \frac{1}{\mathcal{N}} f\left(\frac{N}{2}\right) \exp\left(-\alpha\tau\left(N-1\right)\right). \tag{10}$$

We assume $N = 2^k$, with k an integer. This is obviously true only for a very restricted set of N, but as we are interested on how the distributoin depends on N for large N, looking at these specific points is good enough. Then, by recursion,

$$f(N) \simeq \frac{1}{\mathcal{N}^k} f(1) \exp\left(-\alpha\tau\left(N(1+1/2+1/2^2+...+1/2^k)-k\right)\right). \tag{11}$$

If N is large enough, $1+1/2+1/2^2+...+1/2^k \simeq 2$. Remebering than k was defined as $N = 2^k$, the result is:

$$f(N) \simeq f(1) N^{\frac{\alpha\tau - \log(\mathcal{N})}{\log(2)}} \exp\left(-2\alpha\tau N\right). \tag{12}$$

When $\alpha\tau \gg 1$, links typically break before the next replication, thus there is little impact of the clustering on the growth, and thus the growth will be close to its value in the abscence of clustering, i.e. doubling every τ, thus in this limit $\mathcal{N} = 2$:

$$f(N) \simeq f(1) N^{\frac{\alpha\tau}{\log(2)} - 1} \exp\left(-2\alpha\tau N\right). \tag{13}$$

This rough approximation allows to explain the core of the observed distribution.

5 Model with force-dependent breaking rate

5.1 Model and equations

A link between bacteria may consist of several sIgA bonds, and the number of bound sIgA may not be exactly the same from one inter-bacteria link to the next, but as sIgA are likely well mixed, many per bacteria and that bacteria are similar to each other, let us assume that link heterogeneity is negligible. The links could break if there was some process degrading the sIgA, but the sIgA are thought to be very stable[3]. Another possible explanation for link breaking is that the antigen get extracted from the bacterial membrane, which may depend exponentially with the force applied on the link[4][5]. If the forces are produced by the bacteria themselves (such as by flagella rotation), there are likely to fluctuate on timescales which are short compared to the time between two bacterial replications, and their distribution is likely to be the same for all links, so it would be appropriate to model their effect as a fixed breaking rate, the same for all the links. Another force is the hydrodynamical force exerted by the flow on the bacterial chain.

The flow in the digestive system is complex and not precisely characterized. Longer bacterial chains may also bend and their shape have complex interactions with the flow. Here, we present the simplest model taking into account the forces exerted by the flow on the link breaking rate. We aim to capture the main plausible effects of the flow when the link breaking rate is force-dependent.

Let us take a linear chain of N bacteria, each of length B. Let us approximate it by a rigid chain with beads linked by straight rods of length B (pannel A of

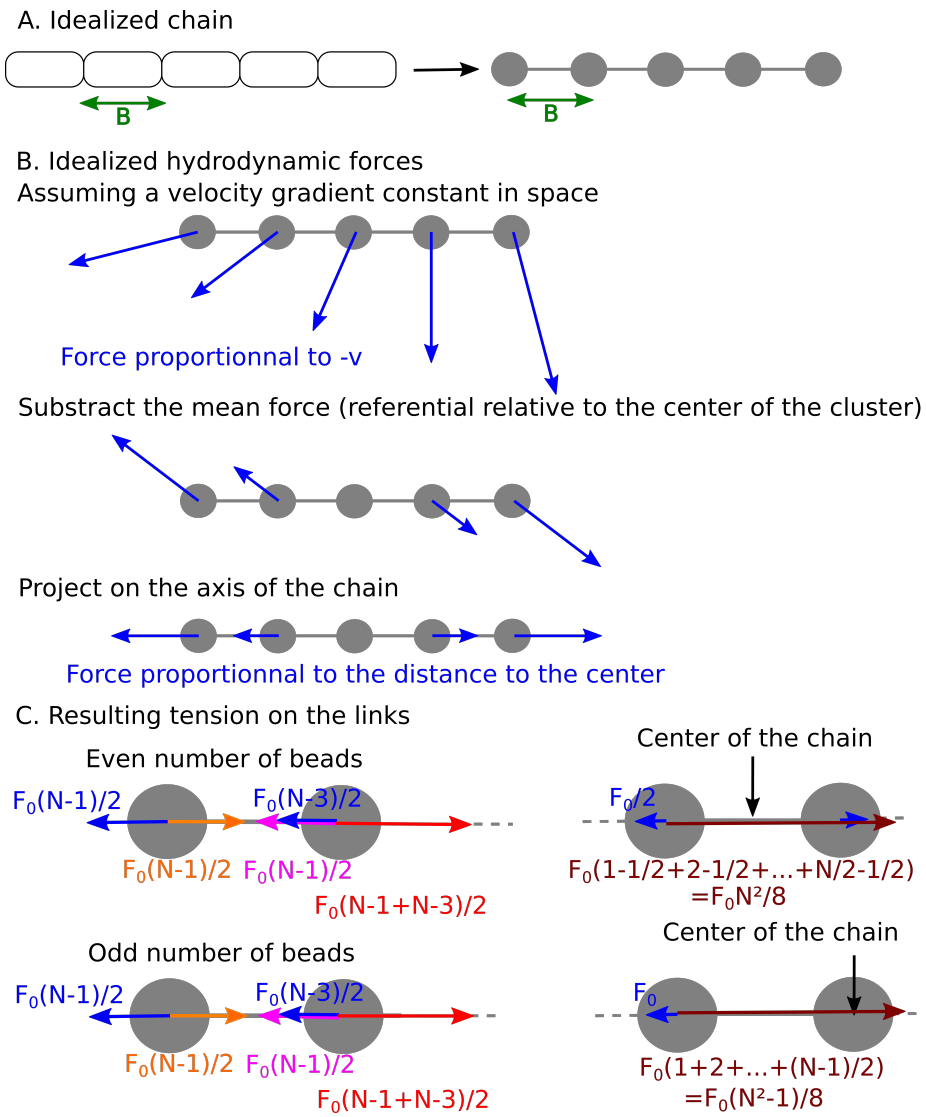

Figure 6: Schematic of the forces applied to the chain. **A** We assume a straight chain of beads with no hydrodynamic interactions between them. **B** We substract the average force to put ourselves in the referential of the center of the chain, as the total force will translate the whole chain and not impact on the forces on the links. We focus on the forces parallel to the chain that will impact the tension between the links. **C** Sum of the forces on each bead, for chains with even and odd number of beads.

figure 6). Let us assume that the rods are infinitely thin so they do not interact with the flow, and let us neglect the hydrodynamical interaction between the beads, so they each are subject to the same frictional force for a given fluid velocity, and, given that the typical Reynolds numbers in the digestive tract are relatively low[6], then the viscous force on each bead is proportionnal to the

flow velocity.

Then, let us assume that the velocity gradient in the fluid is constant around the chain. The rationale for this approximation is that the typical scales of the flow are of the order of the centimeter / milimeter (for instance in a mouse, the cecum typical size is in the cm range), much larger than typical bacterial chains (the length of one bacteria is about $2\mu m$, so even chains of dozens of bacteria remain small compared to the typical flow scale), thus we take a linear approximation of the velocity field in the vicinity of a baterial chain.

Then, if we take the sum of the forces on the whole chain, it will be equal on mN multiplied by the acceleration of the center of mass of the chain, with m the mass of each bead. When all the beads move together, there is no force on the links, thus let us take the referential relative to the center of the chain, and subtract the mean force on each bead (pannel B of figure 6). Then, there remain forces perpendicular to the axis of the chains, and forces parallel to the axis of the chain. The forces perpendicular to the axis of the chain will make it rotate, and as they are perpendicular, they have no effect on the tension on the rods. Then, let us consider only the forces parallel to the chain.

In the example portrayed here, the chain is elongated. The reverse could happen, but in this case, the chain would likely buckle, and the force applied on the links would be small. The flow varies considerably in time, due to peristaltic motions[7][6]. There would be moments with no force and little breaking, and moments with larger forces and more breaking. The flow due to peristaltic motions changes on time scales short compared to the typical bacterial division time, thus we will assume that periods of low breaking and high breaking rates will be equivalent to an average effective breaking rate. Then let us consider the case of elongation only, as portrayed here.

Then the force on each bead is equal to F_0 multiplied by the distance to the center divided by B. We assume, following [4][5], that the breaking rate is dependent on the force. Thus, we define α and β such that the breaking rate of a link is $\alpha \exp(\beta F/F_0)$ if a force F is applied to the link. In the limit of small force, the breaking rate will be α, the same for all links, as in the base model. β is some constant caracterizing how much the stability of the link is force-dependent.

We can write the force on each bead (pannel C of figure 6). Then, here, because the chain is rigid and straight, the sum of the forces on each bead has to be zero. The tension on the outermost link will simply be equal to the flow force on the outermost bead, i.e. F_0 multiplied by its distance to the center divided by B, i.e. $(N-1)/2$ (both for chains of odd and even number of beads). On the next link, the tension has to compensate for the flow force on the second bead, plus the tension applied by the outermost link. Thus the tension on this link is $F_0((N-1)/2+(N-1)/2-1)$, and so forth (this is analogous to modelling of breaking of polymer chains in elongational flows, as in[8]).

For N even, the force on the jth link starting from the outermost link will be:

$$F_{jth\ link,N\ even} = F_0 \sum_{k=N/2-j+1}^{N/2} (k-1/2) \tag{14}$$

Using $\sum_{i=1}^{n} i = i(i+1)/2$, it can be rewritten as:

$$F_{jth\ link,N\ even} = F_0 \left(\frac{N(N+2)}{8} - \frac{(N-2j)(N+2-2j)}{8} - j/2 \right), \tag{15}$$

$$F_{jth\ link,N\ even} = F_0 \left(\frac{N^2}{8} - \frac{(N-2j)^2}{8} \right). \tag{16}$$

There are two links j^{th} away from the extremities, for j from 1 to $N/2-1$, and one central link, for which $j = N/2$. This leads to equation (30) of the main text:

$$\frac{dn_i}{dt} = -rin_i - \alpha n_i \exp\left(\frac{\beta i^2}{8}\right) \left(1 + 2\sum_{j=2}^{i/2} \exp\left(-\frac{\beta}{2}(j-1)^2\right)\right) + r(i-1)n_{i-1} + 2\alpha n_{i+1} \exp\left(\frac{\beta i}{2}\right) \tag{17}$$

For N odd, the force on the jth link starting from the outermost link will be:

$$F_{jth\ link,N\ odd} = F_0 \sum_{k=(N-1)/2-j+1}^{(N-1)/2} k. \tag{18}$$

Simiarly to the N even case, we can rewrite:

$$F_{jth\ link,N\ odd} = F_0 \left(\frac{(N-1)(N+1)}{8} - \frac{(N-1-2j)(N+1-2j)}{8} \right), \tag{19}$$

$$F_{jth\ link,N\ odd} = F_0 \left(\frac{N^2}{8} - \frac{(N-2j)^2}{8} \right) \tag{20}$$

Because of the two sides, there are two links j for each chain, for j from 1 to $(N-1)/2$. Then, this lead to equation (31) of the main text for the evolution in time of the mean number of clusters of odd size i:

$$\frac{dn_i}{dt} = -rin_i - 2\alpha n_i \exp\left(\frac{\beta i^2}{8}\right) \sum_{j=1}^{(i-1)/2} \exp\left(-\frac{\beta}{2}\left(j - \frac{1}{2}\right)^2\right) + r(i-1)n_{i-1} + 2\alpha n_{i+1} \exp\left(\frac{\beta i}{2}\right). \tag{21}$$

5.2 Additional figure for the force-dependent model: replication rate maximizing the growth rate as a function of β

See figure 7.

5.3 Force-dependent model: approximation for the cluster size distribution.

We start from equations (30) and (31), and assume that for t long enough, $n_i \simeq p_i \exp(\lambda t)$ (with λ the largest eigenvalue). Then,

$$\lambda p_i = -rip_i - \alpha p_i \exp(\beta i^2/8)X + r(i-1)p_{i-1} + 2\alpha p_{i+1} \exp(\beta i/2) \tag{22}$$

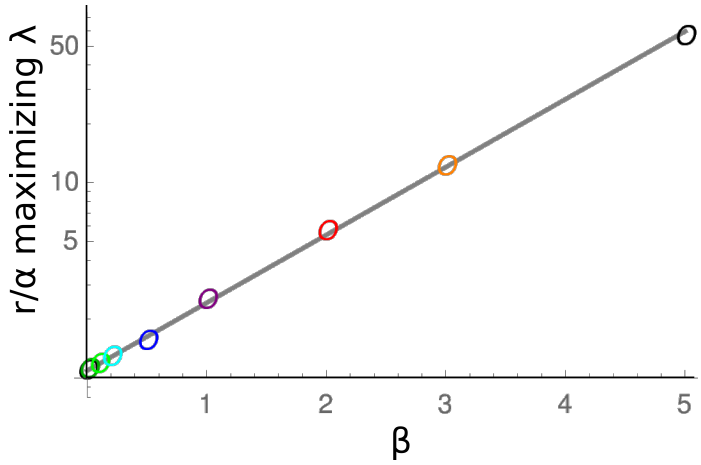

Figure 7: Log of the value of r/α maximizing the growth rate in the force-dependent breaking rate model as a function of β. The points are numerical maximums, the line is $1.09 \times \exp(0.8\beta)$. 1.09 is the value of (r/α) maximizing the growth rate for the base model (i.e. for $\beta \to 0$).

with $X = 1 + 2\sum_{j=1}^{i/2-1} \exp(-\beta j^2/2)$ (i even) or $X = 2\sum_{j=1}^{(i-1)/2} \exp(-\beta(j - 1/2)^2/2)$ (i odd). For i large enough, $\lambda \ll ri$. X will tend to a finite number (converging sum) (to $Y = \theta_3(0, \exp(-\beta/2))$) for i even, $Z = \theta_2(0, \exp(-\beta/2))$) for i odd, and θ_i the Jacobi Theta functions), thus, because β is positive, for i large enough, $ri \ll \alpha \exp(\beta i^2/8)X$. Then we have to determine which of $r(i-1)p_{i-1}$ and $2\alpha p_{i+1} \exp(\beta i/2)$ dominates. If the second one dominates, $\alpha p_i \exp(\beta i^2/8)X \simeq 2\alpha p_{i+1} \exp(\beta i/2)$, thus $p_{i+1}/p_i \simeq \alpha \exp(\beta i(i/8 - 1/2))X$, which for i large enough means that the larger the cluster, the more of it, which would diverge and does not make sense in this system. Thus $\alpha p_i \exp(\beta i^2/8)X \simeq r(i-1)p_{i-1}$,

$$\frac{n_i}{n_{i-1}} \to \frac{p_i}{p_{i-1}} \simeq \frac{r}{\alpha}\frac{i-1}{X} \exp\left(-\beta\frac{i^2}{8}\right). \tag{23}$$

This approximation is valid for large i. Assuming that it is valid for any i,

$$p_{i,even} \simeq \left(\frac{r}{\alpha}\right)^{i-1} \frac{(i-1)!}{Y^{i/2}Z^{i/2-1}} \exp\left(-\frac{\beta}{8}\left(-1 + \frac{i + 3i^2 + 2i^3}{6}\right)\right) \tag{24}$$

$$p_{i,odd} \simeq \left(\frac{r}{\alpha}\right)^{i-1} \frac{(i-1)!}{Y^{(i-1)/2}Z^{(i-1)/2}} \exp\left(-\frac{\beta}{8}\left(-1 + \frac{i + 3i^2 + 2i^3}{6}\right)\right) \tag{25}$$

These two equations can be combined, and ultimately lead to:

$$p_i \simeq \left(\frac{r}{\alpha}\right)^{i-1} \frac{(i-1)!}{Y^{floor(i/2)}Z^{floor((i-1)/2)}} \exp\left(-\frac{\beta}{8}\left(-1 + \frac{i + 3i^2 + 2i^3}{6}\right)\right) \tag{26}$$

5.4 Additional figure for the force-dependent model: cluster size distribution for other values of r/α

See figure 8.

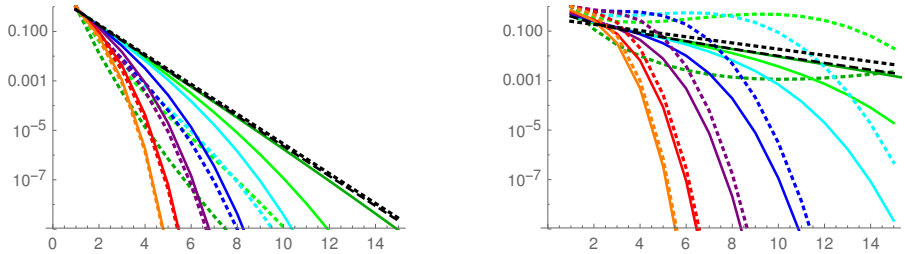

$r/\alpha = 1/3$ $r/\alpha = 3$

Figure 8: Distribution of the cluster sizes, as in figure 2J, except for the value of r/α

6 Experimental data

Mice, which were previously vaccinated with a peracetic-acid inactivated S.Typhimurium strain (PA-S.Tm), were pretreated with 0.8g/kg ampicillin sodium salt in sterile PBS. 24h later, mice received 10^5 CFU of a 1:1 mix of mCherry-(pFPV25.1) and GFP-(pM965) expressing attenuated S. Tm M2702. For imaging, cecum content was diluted gently 1:10 w/v in sterile PBS containing 6μg/ml chloramphenicol to prevent growth during imaging. 200μl of the suspension were transferred to an 8-well Nunc Lab-Tek Chambered Coverglass (Thermo Scientific) and imaged at 100x using the Zeiss Axiovert 200m microscope. To determine the distribution of bacteria in aggregates, n=25 high power fields per mouse were randomly selected and imaged for mCherry and GFP fluorescence. For some mice, sequential sampling was done, these mice were terminally anaesthetised and artificially respirated cecum content was sampled by tying off part of the cecum each hour for 3h. More details about the experimental procedures can be found in [1].

We analyzed all the images for the early data points (4 and 5 hours) of experiments starting from a low inoculum (10^5), to minimize the clustering from random encounters. Only the linear clusters were counted. Images are for the red and green fluorescence, so complex clusters with two colors were not counted. The data was analyzed manually. The images are available upon request.

For linear clusters, we obtained the following distribution : clusters of size 2 (106), 3 (40), 4 (94), 5 (11), 6 (15), 7 (19), 8 (19), 9(1), 10 (2), 11 (1), 12 (2), 13 (2), 14 (1).

The data may be biased, as longer chains may not be fully in the focal plane. Because of gravity, they would fall close to the cover slip. The mass of one bacteria is about one pg, and its density is about 10% more than the water density[9, 10], the thermal energy at ambient temperature is of the order of $4.10^{-21}J$, and gravity g is of the order of $10m/s^2$, thus thermal fluctuations will lift a bacteria by typically 4 μm higher than the bottom. Thus parts of the chains may be out of focus, as this is confocal microscopy, which typical optical section is less than 1μm.

Below, the table of the linear clusters counted on the images from several experiments, either with mice sampled once (o), or with mice sampled sequentially (s).

cluster size	4h PI o (7 mice)	4h PI s (3 mice)	5h PI o (4 mice)	5h PI s (2 mice)	total
2	21	30	17	38	106
3	22	4	9	5	40
4	51	9	25	9	94
5	7	0	1	3	11
6	5	3	3	4	15
7	10	1	5	3	19
8	12	0	4	3	19
9	1	0	0	0	1
10	1	0	0	1	2
11	1	0	0	0	1
12	0	0	1	1	2
13	0	0	1	1	2
14	0	0	1	0	1

7 Recapitulation table of the symbols used

Base model	
r	Bacterial replication rate
α	Breaking rate of the link between two bacteria
$n_i(t)$	Number of linear clusters of length i at t (n_1: free bacteria)
λ	Largest eigenvalue of the matrix, which is the growth rate of the free bacteria in the steady state
Model with bacterial escape and bacterial loss (all these parameters are taken as 0 in the base model)	
δ	When a free bacteria replicates, the probability that this will lead to 2 free bacteria
δ'	When a bacteria at the tip of a cluster replicates, the probability that the daughter cell at the exterior side escapes
δ''	When a bacteria replicates within a cluster, the probability that the daughter bacteria will not be bond to each other, resulting to the cluster breaking in two
c	Loss rate for the free bacteria
c'	Loss rate for the clusters
Model with fixed replication time	
τ	Time between one bacterial division and the next (the bacterial growth rate is $r_{eff} = \log(2)/\tau$)
$\mathcal{N}$	Largest eigenvalue of the matrix in this model. $\mathcal{N} = \exp(\lambda\tau)$
Model with linear chains independent after breaking	
q	Probability that when a inner link of a cluster breaks, the two subparts become independent linear clusters. In the base model, $q = 0$.
Model with force-dependent breaking rate	
β	A constant expressing the strength of the coupling between hydrodynamic forces and link breaking. In the base model, $\beta = 0$.

References

[1] Moor, K., et al. (2017) High-avidity IgA protects the intestine by enchaining growing bacteria. *Nature*, **544**, 498–502.

[2] World Health Organization & Food and Agriculture Organization (2002) *Risk assessments of Salmonella in eggs and broiler chickens*, vol. http://www.who.int/foodsafety/publications/micro/salmonella/en/.

[3] Brandtzaeg, P. (2003) Role of secretory antibodies in the defence against infections. *International Journal of Medical Microbiology*, **293**, 3–15.

[4] Evans, E., Berk, D., and Leung, A. (1991) Detachment of agglutinin-bonded red blood cells. I. Forces to rupture molecular-point attachments. *Biophysical Journal*, **59**, 838–848.

[5] Evans, E. A. and Calderwood, D. A. (2007) Forces and bond dynamics in cell adhesion. *Science*, **316**, 1148–1153.

[6] Lentle, R. and Janssen, P. (2008) Physical characteristics of digesta and their influence on flow and mixing in the mammalian intestine: a review. *Journal of Comparative Physiology B*, **178**, 673–690.

[7] Hulls, C., Lentle, R. G., de Loubens, C., Janssen, P. W., Chambers, P., and Stafford, K. J. (2012) Spatiotemporal mapping of ex vivo motility in the caecum of the rabbit. *Journal of Comparative Physiology B*, **182**, 287–297.

[8] Odell, J. and Keller, A. (1986) Flow-induced chain fracture of isolated linear macromolecules in solution. *Journal of Polymer Science Part B: Polymer Physics*, **24**, 1889–1916.

[9] Bratbak, G. and Dundas, I. (1984) Bacterial dry matter content and biomass estimations. *Applied and environmental microbiology*, **48**, 755–757.

[10] Baldwin, W. W., Myer, R., Powell, N., Anderson, E., and Koch, A. L. (1995) Buoyant density of escherichia coli is determined solely by the osmolarity of the culture medium. *Archives of microbiology*, **164**, 155–157.